Int J Biometeorol (2006) 50: 312–322
DOI 10.1007/s00484-005-0017-4

ORIGINAL ARTICLE

R. Thompson · R. M. Clark

Spatio-temporal modelling and assessment of within-species phenological variability using thermal time methods

Received: 26 November 2004 / Revised: 25 October 2005 / Accepted: 8 November 2005 / Published online: 28 February 2006

Abstract Phenological observations of flowering date, budding date or senescence provide very valuable time series. They hold out the prospect for relating plant growth to environmental and climatic factors and hence for engendering a better understanding of plant physiology under natural conditions. The statistical establishment of associations between time series of phenological data and climatic factors provides a means of aiding forecasts of the biological impacts of future climatic change. However, it must be kept in mind that plant growth and behaviour vary spatially as well as temporally. Environmental, climatic and genetic diversity can give rise to spatially structured variation on a range of scales. The variations extend from large-scale geographical (clinal) trends, through medium-scale population and sub-population fluctuations, to micro-scale differentiation among neighbouring plants, where spatially close individuals are found to be genetically more alike than those some distance apart. We developed spatio-temporal phenological models that allow observations from multiple locations to be analysed simultaneously. We applied the models to the first-flowering dates of *Prunus padus* and *Tilia cordata* from localities as far apart as Norway and the Caucasus. Our growing-degree-day approach yielded a good fit to the available phenological data and yet involved only a small number of model parameters. It indicated that plants should display different sensitivities to temperature change according to their geographical location and the time of year at which they flower. For spring-flowering plants, we found strong temperature sensitivities for islands and archipelagos with oceanic climates, and low sensitivities in the interiors of continents.

Keywords Phenology · Temperature threshold · Growing degree-day · Clinal variation · Linear statistical model

R. Thompson (✉)
School of GeoSciences, The University of Edinburgh,
Edinburgh, UK
e-mail: roy@ed.ac.uk
Fax: +44-131-6683184

R. M. Clark
School of Mathematics, Monash University,
3800 Vic, Australia

Introduction

Under field and laboratory conditions, temperature is generally found to be a primary determinant of the dates of first flowering (FFD) and the rate of leaf appearance in plants (e.g. Salisbury 1963; Hodgson 1978), while other effects, including radiation, photoperiod and rate of change of photoperiod, have also been found to be of significance (e.g. Baker et al. 1980; Myers et al. 1982; Slafer and Rawson 1994; Slafer and Rawson 1995; Bertero 2001). In many trees of temperate origin, springtime warmth advances the date of budding and flowering (Fitter et al. 1995); however the degree of chilling during winter is also known to affect the thermal time required for budburst (Murray et al. 1989; Hänninen 1990; Heide 1993). In several temperate tree species, insufficient winter chilling is found to delay budburst (e.g., Murray et al. 1989; Falusi and Calamassi 1990). Inflorescence formation may also be influenced by chilling (Cesaraccio et al. 2004; De Melo-Abreu et al. 2004) in temperate species. In the natural environment, plants are subjected to a wide variety of climatic and meteorological phenomena that fluctuate from one year to the next, and the resulting biological behaviour can display pronounced inter-annual fluctuations. By analysing observations of ontogenetic plant development over a series of years (e.g. time series of the dates of first flowering) and by making careful comparisons with potential explanatory factors (e.g. radiation, temperature), phenological models can be constructed linking plant and climatic behaviour. The growing prospect of significant climate change over the coming century (IPCC 2001), e.g. average temperature increases of several degrees Celsius coupled with changes to both the intensity and the

seasonality of precipitation, foreshadows the increasing likelihood of profound changes to the growth patterns of plants in the natural environment. Statistical analysis of phenological data holds out the prospect for quantitative calibration of the effects of climate on plant behaviour and for assessing the future impact of climate change on plant growth and ontogenetic development (e.g. Menzel and Fabian 1999; Fitter et al. 1995).

A spring warming model for the timing of phenological phases was first introduced by the French physicist Rene de Reaumur (1735). Reaumur's approach was extremely simple. He summed daily air temperatures (after an arbitrary start date) and found the totals were related to the stage of a plant's development. The great French naturalist Michel Adanson adapted Reaumaur's idea by disregarding all temperatures below 0°C and summing only the positive temperatures. He showed foresight in his conviction that a heat-unit approach could be used to tell when certain plants would germinate, flower, or release their pollen. Cumulative cooling degree-days are similarly used today by heating engineers to schedule air-conditioning inside buildings. Despite its apparent simplicity, the heat-unit approach continues to be widely used in agronomy, entomology and horticulture (Trudgill et al. 2005). In trees, the initiation of the growing season has been successfully modelled using a cumulative thermal summation (e.g., Thomson and Moncrieff 1981; Cannell and Smith 1983). As noted above, certain tree types must fulfil a chilling requirement before warmer temperatures begin to affect springtime growth, and some models include this parameter (e.g., Landsberg 1974; Hänninen 1990; Chuine et al. 1998; De Melo-Abreu et al. 2004; Cesaraccio et al. 2004).

A common restriction to the establishment of durable phenological models is that, as the model has to be tuned for each individual species, variety or cultivar, the number of available data points is often low (as only one data point is obtained for each year of recording). We describe a degree-day procedure that allows observations from any number of geographical localities, but for a single species, to be aggregated. Even solitary observations from a single year, at just one locality, can be incorporated into our procedure. So the total number of observations used in our model building can be reasonably large. We apply the method to a data set with 1,706 observations of *Prunus padus* and also to a data set with 294 observations of *Tilia cordata*.

Populations of a single species may diverge genetically (Epperson 1993; Epperson and Clegg 1986) owing to local adaptations to changes in climate or environment (Escudero et al. 2003), or to genetic drift (Heywood 1991). The resulting geographical variation within a species (e.g. of

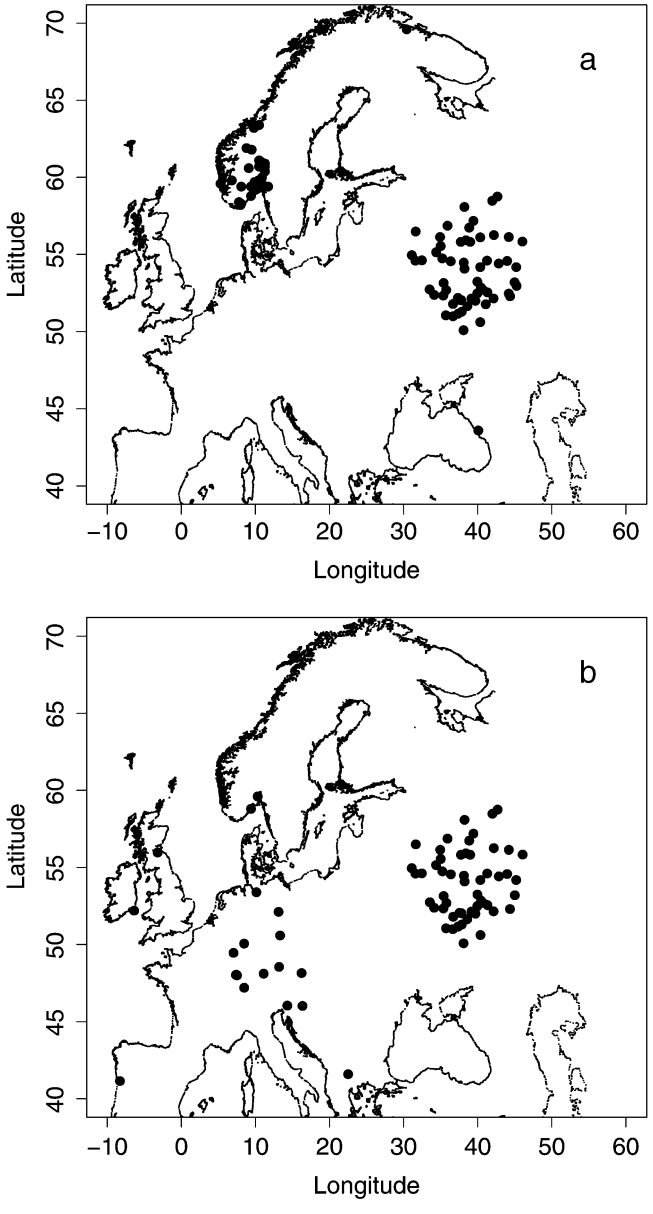

Fig. 1 Map of the distribution of observation stations for **a***Prunus padus* and **b***Tilia cordata*

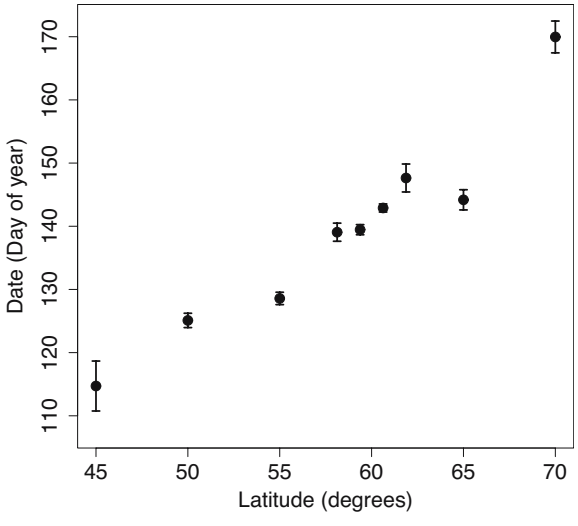

Fig. 2 First-flowering date vs. latitude for *Prunus padus*. Each *symbol* plots the main flowering date for all observations within 13 latitude bands. The *error bars* depict the associated 95% confidence limits

biomass, height, or seed production) is often gradual (i.e. clinal). For example, for the over-wintering of birch, Welling et al. (2004) reported a clinal pattern to the induction of dormancy during autumn, when photoperiod has a determining role, but in contrast found no clinal variation in the spring as the release of dormancy is regulated by temperature. Our degree-day model allows us to statistically assess whether there is any evidence for clinal variation in phenological thresholds.

The main practical objective of this work was to evaluate the relative importance of temperature, photoperiod (obligatory) and geographical effects in phenological models of the first flowering of *Prunus padus* and *Tilia cordata*, and hence to make predictions of the likely impact of global warming on their flowering behaviour.

Materials and methods

First-flowering observations

We gathered together first-flowering observations for the two species *Prunus padus* and *Tilia cordata* from localities across Europe (Fig. 1). Our earliest observation was from 1906 in the Royal Botanic Garden, Edinburgh. Many observations were obtained from the network of the International Phenological Gardens (IPG), a European network first established in 1959 (Chmielewski 1996). Other first-flowering dates were taken from the Lauscher and Printz (1955) phenological network in Norway. *Prunus padus* data were also taken from the Russian plains database (Minin 2000). Figure 2 groups the *Prunus padus* FFDs into 2.5-degree or 10-degree latitude bins and shows an increasing lateness of flowering with latitude.

Prunus padus, the European birdcherry, is an attractive, low-branched, deciduous, ornamental tree that typically grows 8–19 m tall with a rounded crown. Small, white, fragrant flowers in pendulous 7- to 20-cm-long clusters (racemes) appear after the foliage emerges in spring. Flowering occurs on the previous season's wood. *Prunus padus* is frost tolerant in both spring and autumn and is entomophilous (insect pollinated), usually by flies. At our sites, first-flowering dates varied from late March at 44° S to the end of July at 70° N.

Tilia cordata, the small-leaved lime, is a large, deciduous, broadleaf tree; in woodlands it grows up to 30 m high. It can live 1,000 years under certain conditions. This generally deep-rooted species is scarcely affected by short periods of drought. Pale yellow-white, fragrant, five-petalled flowers form in clusters of 4–15. The inflorescences are borne on stalks coming from axillary buds on the extension shoot of the current year. Flowering typically takes place some 3 months after bud swelling. *Tilia cordata* is a major source of pollen for *Bombus lucorum*. At our sites, first-flowering observations ranged from early April at 41° S to as late as early August at 60° N.

Meteorological data

Next we obtained meteorological data for all the geographic localities at which the FFDs had been observed. The data were based on the high-resolution climate grids created by T. D. Mitchell, and made available through the Climatic Research Unit and Tyndall Centre. We used the CRU TS 1.2 data set (Mitchell et al. 2004) that covers the European land surface at a 10-min resolution, at monthly intervals during the period 1901–2000. In order to generate tem-

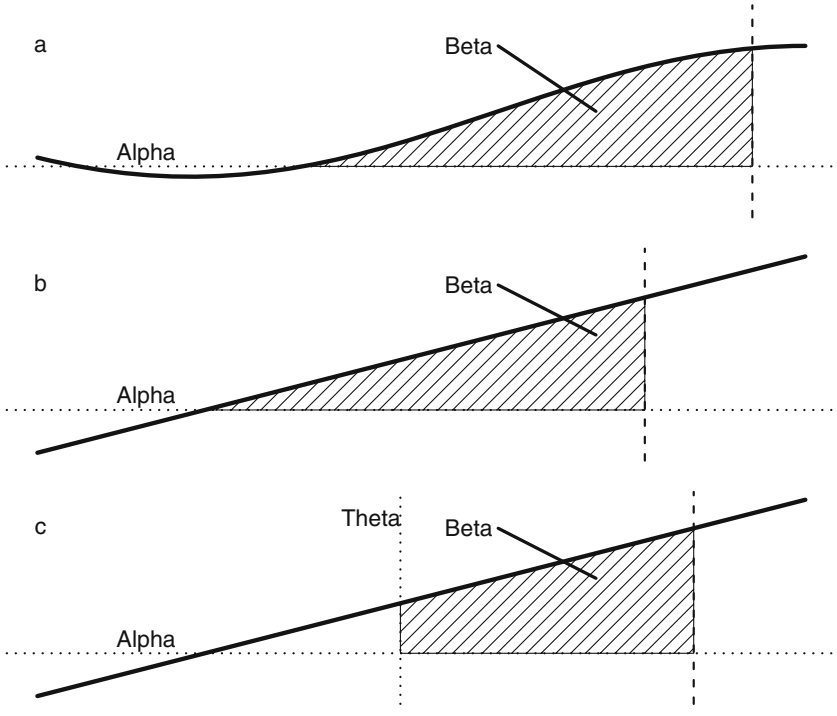

Fig. 3 Schematic diagrams illustrating growing-degree-day thresholds and requirements. **a** Sine-curve model. **b** Straight-line two-parameter growing-degree-day model. **c** Straight-line three-parameter growing-degree-day model

peratures for each location and year of our FFD observations, a lapse rate correction procedure that allowed site altitude to be taken into account was combined with a linear interpolation scheme and applied to the climate grid. The monthly mean temperatures were then used to calculate a linear rise in spring temperature for each year at each locality. Our sites span a wide climatic range. The *Prunus padus* sites encompass regimes with summer monthly mean air temperatures that vary from 10–23°C, and winter regimes from −20 to +4°C. The *Tilia cordata* sites encompass regimes with summer temperatures that vary between 13 and 25°C, and winter temperatures that range from −15 to +8°C. At any one site, the year-to-year (inter-annual) variations are highest in winter (typically around 12°C for the *Prunus padus* sites and 10°C for the *Tilia cordata* sites); while in summer, the year-to-year variations are typically about 6°C at the *Prunus padus* sites, and 8°C at the *Tilia cordata* sites.

Phenological models

Once we had obtained these extensive data sets of first-flowering dates and the month-by-month progression of the weather, our next task was to examine whether there was any relationship between FFD and weather, and if so, what the relationship was. We also wanted to be able to determine if there was any dependence of the relationship on geographic location (e.g. latitude or longitude). We used the growing-degree-day (GDD) approach (described above) as our starting point in formulating equations that related the date of first flowering to meteorological and geographical parameters. Figure 3 illustrates how the thresholds in GDD models take the form of thermal limits (e.g. minimum temperature), or temporal limits (e.g. photoperiod, ratio of day length to night length). GDD accumulation works as follows. Once the photoperiod threshold (theta) is passed, GDDs can begin to be accumulated. Suppose on a particular day that the threshold temperature (alpha) has been exceeded, then the difference between the average temperature and the threshold gives the GDDs for that day. Then on the following day an aggregated temperature sum is calculated by adding the GDDs for that day to the previous total. This cumulative procedure continues, with days colder than the threshold temperature being ignored, until the GDD requirement (beta) for flowering is reached, at which time the plant bursts into bloom. A general approach to GDD modelling is described in the Appendix.

Our aim was to formulate simple equations relating threshold temperature and 'thermal energy' requirements to flowering, in such a way as to be able to describe current behaviour and to allow us to predict the likely, or expected, FFD for any temperature-sensitive species under any future climate regime. A valuable consequence of the simplicity of our heat-unit equations is that they can be easily expanded to handle spatial, as well as inter-annual variations. Spatial aspects are introduced by allowing alpha, beta and theta to vary linearly with position (e.g. latitude or longitude). This facility for handling spatial data applies to all of our models and is described in more detail in the Appendix.

Three types of GDD model emerged

Model 1

We began by considering a 'no skill' or null hypothesis. We use the deviation of first-flowering dates about the mean as a measure of no skill. Our model 1a represents the situation where the day of the year is the only control on first flowering. Our model 1b is extended to incorporate latitude. It represents the situation where a single threshold (e.g. photoperiod) is allowed to vary in a linear manner.

Model 2

Here we note that meteorological data in temperate regions commonly follow an annual cycle. In many GDD formulae, plants aggregate temperature over extended periods. So a sine fit to the annual march of temperature in any given year provides an attractive starting point. However, it is well known that the line $y=x$ is tangent to the graph of $\sin(x)$, so the difference between x and $\sin(x)$ is

Table 1 Temporal *Prunus padus* models based on March, April and May air temperatures. Coefficients, ±1SE and summary statistics

Model	Model number	θ (Julian day)	α (°C)	β* (degree-days)$^{1/2}$	Residual SE (days)	Mad (days)	Bias (days)	df
Photoperiod	1a	140±0.3	–	–	12.5	9.3	0.00	1,705
Growing degree-days	2a	–	2.55±0.15	13±0.28	7.0	5.1	0.02	1,704
Accumulated temperature	2b	99±1.5	0.36±0.18	16±0.08	6.8	5.0	−0.07	1,703
Photo +degree-day	2c	91±2.2	0.03±0.22	17±0.07	6.7	4.9	−0.04	1,703

Df Degrees of freedom, *Mad* mean absolute deviation, *Bias* mean residual, θ daylight threshold, α thermal threshold, β growing degree-day threshold

Note: The phenological models are linear in sqrt(β), hence the use of β* = sqrt(β). However this means that the classic methods for getting confidence limits do not apply when the estimated betastar is negative or close to zero

Table 2 Spatio-temporal *Prunus padus* models based on March, April and May air temperatures. Coefficients, ±1SE and summary statistics

Model	Model number	θ_{60} (Julian day)	θ_{lat} (Julian day per degree lat)	α_{60} (°C)	α_{lat} (°C per degree lat)	β^*_{60} (degree-days$^{1/2}$)	β^*_{lat} (degree-days$^{1/2}$ per degree lat)	Residual SE (days)	Mad (days)	Bias (days)	df
Photoperiod	1b	143±3.1	2.2±0.05	–	–	–	–	8.8	6.7	0.00	1,704
Growing degree-days	3a	–	–	3.1±0.5	−0.51±0.04	12.3±0.27	0.74±0.08	6.6	4.9	0.04	1,702
Accumulated temperature	3b	107±2.0	3.5±0.61	1.2±0.20	0.27±0.09	16.4±0.11	−0.05±0.02	6.4	4.7	−0.02	1,700
Photo + degree-day	3c	108±1.8	3.1±0.52	1.3±0.19	0.21±0.08	16.3±0.11	−0.04±0.016	6.4	4.7	−0.03	1,700

Symbols as in Table 1
The *subscript 60* indicates that the coefficient has been evaluated at the latitude 60°N. The latitude 60°N is used because it is the average latitude of the 1,706 first flowering observations
The *subscript lat* denotes variation with latitude

very small when x is close to zero [and the phase of sin(x) is zero]. This suggests that representing temperature change by a straight line rather than a sine curve could, under suitable conditions, be very effective. The Appendix considers such a straight-line formulation, while Fig. 3 sets out its key geometrical features. There are three variants to consider. The simplest model, 2a (Fig. 3b), involves just a temperature threshold (alpha) and a growing-day requirement (beta). Here, given a suite of FFD observations and monthly (or daily) climate data, both parameters can be derived directly using classic least-squares regression (see Appendix). Such a regression set-up has many advantages. In particular it allows confidence limits to be established and places the model within a well-established linear framework. Rather than just aggregating temperatures above a threshold, and ignoring temperatures below the threshold, a second approach (model 2b) is to use the threshold as a base level and to total up temperatures both above and below the base-line. We refer to model 2b as the accumulated-heat-unit model. The accumulated-heat-unit approach (e.g., Degrandi-Hoffman et al. 1996) needs a photoperiod threshold, and so it is a three-parameter model. The third variant (model 2c) is a three-parameter GDD model. The three parameters are a photoperiod threshold, a temperature threshold and a total energy (GDD) requirement. Figure 3c provides a geometrical representation of model 2c. In model 2 some care is needed in the estimation of alpha and beta because of the constraint that beta must be positive. The main difficulty concerns the estimation of confidence limits when beta is close to zero. Various approaches to overcoming this problem are possible; one is noted in the Appendix.

Model 3

The final group of models we considered incorporate geographical controls as predictors. A spatial effect (e.g. latitude) is added to the simple regression set-up of model 2. This spatial aspect of the modelling is achieved by allowing alpha, beta and theta to vary linearly with latitude. This set up applies to all variants of model 3. As with model 2, there are three variants to model 3. These again involve a model with just a temperature threshold plus a growing-day requirement (model 3a); an accumulated-heat-unit model (model 3b); and a three-threshold straight-line model (3c) that combines a photoperiod plus a temperature threshold with a GDD requirement. A drawback to the type-3 models is that they are intrinsically nonlinear. Nevertheless the method of Bates and Chambers (1992) allows nonlinear least-squares estimates of the nonlinear model parameters to be determined, along with appropriate confidence limits.

Table 3 Temporal *Tilia cordata* models based on March to June air temperatures. Coefficients, ±1SE and summary statistics

Model	Model number	θ (Julian day)	α (°C)	β^* (degree-days)$^{1/2}$	Residual SE (days)	Mad (days)	Bias (days)	df
Photoperiod	1a	178±0.9	–	–	15.2	11.1	0.00	293
Growing degree-days	2a	–	3.4±0.6	28.2±1.0	11.2	7.8	0.01	292
Accumulated temperature	2b	123±10	5.9±1.0	39.2±0.4	11.0	7.8	−0.19	291
Photo + degree-day	2c	123±10	5.9±1.0	39.2±0.4	11.0	7.8	−0.19	291

Symbols as in Table 1

The general nature of all our models means that they are easily programmable in any computing language. Furthermore they are readily applicable to other taxa and geographical regions.

Results

Each of the eight models described above has been applied in turn to our *Prunus padus* and *Tilia cordata* data sets. Results from all the models are described below. The model 1, model 2 and model 3 results are set out in some detail in Tables 1, 2, 3 and 4.

Prunus padus

We now briefly describe the results of each model. We begin by considering model 1a. It had a residual standard error of 12.5 days when applied to the 1,706 *Prunus padus* observations. The next model to be examined was the GDD model (model 2a) based on a straight-line fit to the spring temperature rise. It performed much better, yielding a residual standard error of 7.0 days (Table 1). It had a thermal threshold of 2.6°C and a (thermal time) requirement of 13 degree-days.

The many advantages of the linear model set-up, combined with the very satisfactory goodness of fit, of model 2a encouraged us to proceed to investigate the variants of model 2. The results are summarised in Table 1. All three variants yielded very similar fits and all were significant improvements over the null model. The residuals, bias and goodness-of-fit measures of the type 2 models were all virtually indistinguishable from one another (Table 1). As our approach allows observations from many localities to be combined together, we had large data sets with which to work, and as a consequence, we were able to obtain tighter confidence limits on phenological GDD parameters than have been determined previously. Alpha, the thermal threshold, was determined to closer than a quarter of a degree, while the associated GDD requirement was determined to within a third of a degree-day. Furthermore our formulation allowed the joint confidence limits to be explored. Figure 4 plots the joint 95% confidence 'ellipse' for the thermal threshold and the GDD requirement of model 2a. The parameter estimates were, as would be expected, highly correlated. A low temperature threshold was associated with a high degree-day requirement and vice versa. It was this pairing that led to the elongated elliptical shape of Fig. 4.

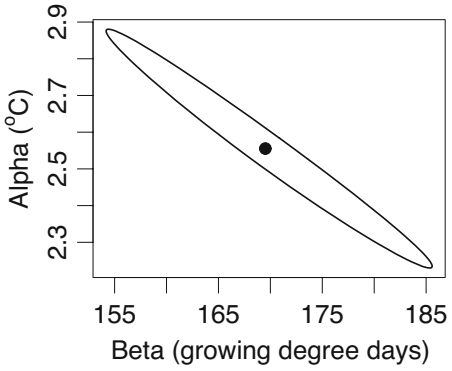

Fig. 4 Joint confidence limits on alpha (the thermal threshold) and beta (the growing-degree-day requirement) for the first flowering of *Prunus padus*. The very slight banana shape of the confidence 'ellipse' arises from the square root of the growing-degree-day term used to linearise the underlying equation (see Appendix)

Emboldened by the internal consistency of the type 2 models and the tight control they offer on the parameter estimates, we went on to investigate the type 3 models. Table 2 sets out the main results from this part of our study. There are three additional parameters to consider, namely the latitudinal effects associated with theta, alpha and beta. Once again goodness-of-fit and residual measures are presented for each fit (Table 2), along with the standard errors of the model parameters. Inspection of Table 2 shows that the geographical parameters were formally significant (the coefficients were typically three to six times as large as their associated standard errors). In addition $theta_{lat}$ showed

Table 4 Spatio-temporal *Tilia cordata* models based on March to June air temperatures. Coefficients, ±1SE and summary statistics

Model	Model number	θ_{54} (Julian day)	θ_{lat} (Julian day per degree lat)	α_{54} (°C)	α_{lat} (°C per degree lat)	β^*_{54} (degree-days$^{1/2}$)	β^*_{lat} (degree-days$^{1/2}$ per degree lat)	Residual SE (days)	Mad (days)	Bias (days)	df
Photoperiod	1b	179±12	1.9±0.2	–	–	–	–	13.6	10.0	0.00	292
Growing degree-days	3a	–	–	2.6±0.6	0.09±0.11	29.5±0.98	−0.52±0.23	10.3	7.2	0.00	290
Accumulated temperature	3b	86±11	−11±2.6	2.4±1.3	−2.1±0.24	33.3±0.21	−0.42±0.05	10.2	7.4	−0.01	288
Photo + degree-day	3c	37±53	212±16	−0.14±4.3	−3.5±1.6	33.7±0.19	−0.4±0.04	10.1	7.4	−0.13	288

Symbols as in Table 1
The *subscript 54* indicates that the coefficient has been evaluated at the latitude 54°N. The latitude 54°N was used because it is the average latitude of the 294 first flowering observations
The *subscript lat* denotes variation with latitude

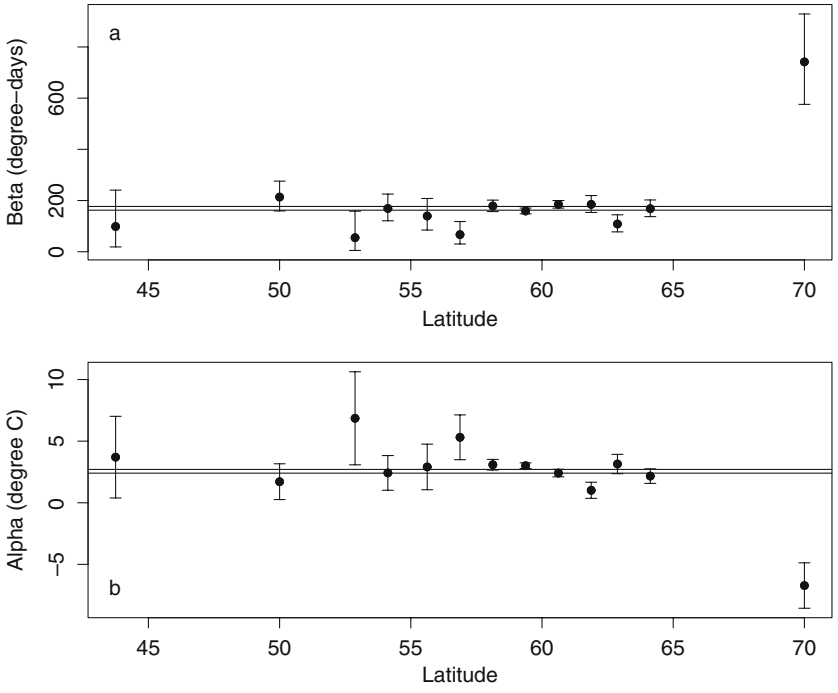

Fig. 5 Latitudinal dependence of **a** beta (the growing-degree-day parameter) and **b** alpha (the thermal threshold) in the phenological model 2c for the date of first flowering of *Prunus padus*. *Error bars* (±1 SE) are shown for the same latitude bands as used in Fig. 2.The *horizontal lines* correspond to the fit to the complete data set and show ±1 SE about the fit. Apart from the most northerly band, the plots shows that, at most, only a small variation in beta or alpha is found with latitude. The expected inverse correlation between individual estimates of alpha and betastar is evident. Although the latitude band at 70° N might at first sight appear anomalous, we note that in this type of analysis it would not be unexpected for one out of the thirteen bins to fall 2 SE from where the "true" alpha and beta might lie

consistency by being positive in all models; that is, the date on which temperatures begin to be accumulated becomes later the further north one goes. By contrast the $\text{alpha}_{\text{lat}}$ and beta_{lat} coefficients did not have the same signs in all models, and so should be viewed with caution. Other attempts we made at discerning a geographical variation, e.g. by using longitude or distance from the sea, produced no further improvements.

In summary many of the models tested on the *Prunus padus* data set produced very similar goodness-of-fit measures. The simplest of these models is the two-parameter GGD model (Fig. 5) with a straight-line fit to the springtime temperature rise (model 2a). As such it represents a viable model for describing present-day first-flowering behaviour and for prediction work.

Tilia cordata

Tables 3 and 4 present the main results of applying the suite of models described above to the *Tilia cordata* data set. The only difference in the analyses from the *Prunus padus* study was that June temperatures were used to extend the period over which the temperature rise was estimated as *Tilia cordata* tends to flower later than *Prunus padus*.

Once again we found that all the models using degree-day or accumulated heat units performed better than the null model. They consistently reduced the residual standard error from 15.2 days to between 10.1 and 11.2 days. On account of the lower number of *Tilia cordata* observations than *Prunus padus* observations the standard errors were naturally wider. Nevertheless the errors for all the type 2 models were once again small (see Table 3), and all the type 2 models showed good internal agreement with each other.

In contrast to the type 2 models, the type 3 models were disappointing as they displayed many differences between one another. For example $\text{theta}_{\text{lat}}$ varied between 1.9 and −212. Such a lack of consistency is a sign of over-fitting. Another indicator of problems with the type 3 modelling was that some of the standard errors approached the size of the parameter estimates (e.g. $\text{alpha}_{\text{lat}}$ in row 4 and beta_{lat} in row 2 of Table 4).

In short, we found the three type 2 models to be the most attractive models for *Tilia cordata*. All these type 2 models demonstrated a temperature effect, with the two-parameter GDD set up of model 2a performing as well as any. Its thermal threshold of 3.4°C and thermal requirement of 28°C degree-days (model 2a in Table 3) were both higher than the equivalent parameters in the corresponding *Prunus padus* model (model 2a in Table 1) as a consequence of the later flowering dates.

Discussion

Our models are very simple and so naturally are only an approximation of the very complex interaction between plants and the weather. Nevertheless our analyses suggest that the models can serve as a reasonable first approximation. Model 2a performs as well as any of the models. This two-parameter model, based around a linear fit to the springtime temperature rise, a thermal threshold and a minimum GDD requirement, is worth exploring in a little more detail. Inspection of the underlying equation (Eq. 6 in the Appendix) provides an insight into the workings of the model. Flowering date appears on the left-hand side of the equation, and temperature on the right. The relationship between flowering date and temperature is most easily understood by taking the partial derivative of μ in Eq. 6

with respect to initial temperature c. This partial derivative measures the effect of a uniform increase in temperature. The differentiation leads to a very simple relationship, namely the sensitivity of flowering date (μ) to temperature (T) is proportional to the inverse of the slope (m) of the springtime temperature rise and we have

$$d\mu/dT = -1/m$$

A number of consequences follow.

First, at any given locality the sensitivities of *Prunus padus* and *Tilia cordata* are, by and large, the same. Indeed under model 2a, at any particular locality, all plants that are responsive to springtime temperatures (no matter what their thermal requirements) have essentially the same sensitivities.

Secondly, because the rate of springtime temperature rise varies from locality to locality, $-1/m$ also varies, and so flowering sensitivity must differ from locality to locality. For example, if we apply model 2a to the observation localities of Fig. 1, then we find temperature sensitivities range from −14 days per degree, at the maritime sites in Ireland, Scotland and Iberia (Fig. 1a), to less than −3 days per degree, at the most easterly (continental) site (Fig. 1b). The negative signs on the sensitivity values indicate that flowering date becomes earlier as temperatures increase.

Thirdly we can use the sensitivities to calculate the effect of an overall change to the climate. For example, if the climate were to cool by 2° (i.e. all months were on average to became 2° cooler than at present) then the change to flowering date would be $+2/m$. Thus all temperature-sensitive plants in the maritime localities of Fig. 1 would flower 28 days later, while exactly the same species at the most continental site of Fig. 1 would, when subjected to exactly the same 2° cooling, flower 6 days later.

Fourthly other empirical phenological models, derived by time-series methods (e.g. Abu-Asab et al. 2001) or regression techniques (e.g. Fitter et al. 1995; Fitter and Fitter 2002), quite often favour inverse temperature relationships, such that a warm spring can give rise to certain species flowering later. Similarly a warm autumn will normally be modelled as causing most species to flower earlier, but the occasional species to flower later (Sparks et al. 2000). Our two-parameter type 2a model can only encompass this type of inverse behaviour if beta is allowed to be imaginary. If beta is constrained to be real (and non-negative) then such species have to be categorised as displaying a very large natural variability unconnected to temperature.

Fifthly in our models the sensitivity of flowering date to temperature depends in a regular fashion on the time of year at which the flowering takes place. The lowest sensitivities occur during mid/late spring, when the accumulation of GDDs is taking place at the time when seasonal temperatures are changing most rapidly.

Turning to a consideration of our adoption of a linear rise in temperature in the spring, we also investigated a fourth model in which a sine fit to the annual march of temperature in any given year was used instead. A sine-function model appears attractive as it involves few empirical parameters and yet can be expected to capture much of the temperature variation. For each year and for each locality, the daily temperature, through the time period of interest—early spring to early summer—was summarised by just three numbers: the phase and amplitude of the sine curve and its overall mean level. We took the period of the sine curve to be 365.25 days. In some years, the mean temperature in early spring was relatively low; in other years relatively high. In some years, temperature increased slowly, in others more quickly. But in all cases we found that springtime temperature variations could be summarised well by just the three numbers of that year's sine function. We next assumed that each species has its own fixed photoperiod threshold (theta), temperature threshold (alpha) and total GDD (beta) requirement. All three are initially unknown but can be estimated from a simple sine equation (see Appendix). The problem is one of determining the best combination of theta, alpha and beta (the three thresholds illustrated in Fig. 3c), i.e. the combination that minimises the squared differences between the observed and the modelled FFDs. This problem turns out to be equivalent to a central conundrum in celestial mechanics: the well-known and much-studied Kepler problem of the motion of two bodies interacting gravitationally. Despite having been studied for over three centuries no exact analytical solution has ever been found (Colwell 1993). Nevertheless a number of technically satisfactory solutions are long established. There are two main strategies to solve Kepler's equation: (1) by an iterative or trial-and-error method, or (2) by obtaining a series. The latter method is known as the 'equation of the centre'. We adopted the first strategy. In practise we found no improvement over the linear approach of model 2. For the *Prunus padus* data set, the sine function, fit to the springtime temperature rise, generated a residual standard error of 7.7 days. The thermal threshold was 4°C, and the growth (thermal time) requirement was 4 degree-days. A three-parameter sine-function fit to the 294 *Tilia cordata* observations similarly generated no improvement in fit over and above that of the straight-line model (2a). Although the sine models were not found to be advantageous in this study, one can envisage situations in which they could be of value. In particular the sine model can deal with phenological events taking place at any time during the year. So the sine model would be expected to out-perform the straight-line models for late-winter and late-summer phenological events. Also for predictive purposes, while our straight-line type-2 and type-3 models can cope with future temperature changes of a few degrees, they should not be pushed too far. Extrapolations to temperature regimes of say five, or more, degrees different from the present day are likely to be better handled by the sine model.

Finally we take the good performance of the type-2 models, which have no within-species clinal variation (Fig. 5), to indicate that our basic type 2a model can be used over a wide range of geographical situations. In the trade-off between simplicity of the model versus residual errors, we have opted for a small number of parameters. This choice is particularly useful in enhancing the ability of a model to predict the effects of global warming. Our model 2a, which only requires two parameters, predicts that at any given locality the great majority of plants will, with climate change, modify their average flowering times in a closely coordinated fashion, while the greatest sensitivities to average flowering date will be found on islands and archipelagos with hyper-oceanic climates.

When using past variations to model plant behaviour, and when trying to forecast the impact of future climate change, caution must be exercised (Theurillat and Guisan 2001) especially if the future change is likely to lie well outside the range of the present-day climate. For example, temperate northern-hemisphere plants already at the southern edge of their range may experience temperature extremes in summer which exceed critical physiological thresholds, or be deprived of essential chilling requirements in winter, as global warming sets in. However as our spatio-temporal models are able to encompass flowering behaviour from a wide climatic range, they are likely to contain useful information for the assessment of future impacts.

Conclusions

- Our linearized growing-degree-day and accumulated-heat-unit models allow phenological results from multiple locations to be combined.
- Flowering dates of *Prunus padus* and *Tilia cordata* were noted as being later in more northerly regions of Europe. While this effect can be modelled by a latitudinal control on a photoperiod threshold, phenological models involving thermal thresholds were found to provide a better fit.
- The accumulated-heat-unit models and growing-degree-day models performed equally well.
- For predictive purposes, a growing-degree-day approach, in combination with a sine-curve or linear approximation of the increase in springtime temperatures, provided an attractive starting point. These approaches yielded a good fit to first-flowering data and yet involved only a small number of model parameters.
- The flowering phenologies of *Prunus padus* and *Tilia cordata* displayed low levels of phenotypic plasticity. No significant changes in their thermal thresholds or growing-degree-day requirements were found across a 10 million km^2 region of Europe, although there was an obvious dependence of FFD on latitude as shown in Fig. 2.
- While much conventional wisdom holds that future climate change, in tandem with the diverse range of weather–flowering relationships previously discovered, will result in plant and animal behaviour becoming dangerously asynchronized, our growing-degree-day / linear springtime temperature model forecasts quite a different situation. It predicts that at any given locality the majority of spring-flowering plants, despite their varied thermal thresholds, will modify their average flowering times in a harmoniously coordinated fashion.
- Our models further forecast that plants of a particular species will modify their flowering behaviour in different ways when subjected to the same degree of climate change if they are growing in different climatic regions.
- Our approach indicates that the greatest sensitivities of springtime flowering dates on temperature are most likely to be found in the hyper-oceanic climates of islands and archipelagos.

Acknowledgements We are indebted to Tim Mitchell for making the high-resolution climate grids available to us; to Gina Clarke for helping us obtain the Norwegian data; and to Joe Monaghan for pointing out the equivalence of our basic GDD sine model with Kepler's equation. The Royal Society of Edinburgh kindly helped facilitate a study visit by RT to Monash University, allowing our analyses to be carried out.

Appendix: General approach to GDD models

Definitions:

$g(x)$ = (mean) temperature on day of year x
α = threshold temperature
β = required growing degree-days
γ = Day of year when the temperature first reaches α
μ = 'theoretical' or 'expected' FFD under the GDD model
θ = photoperiod limit (Julian day when the plant first 'wakes up from hibernation')

For simplicity we consider the relationships for a single year.

General approach

We assume that $g(x)$ is a monotonic, increasing, continuous and one-to-one function. This means that the 'first day', γ, is unique, and must satisfy the equation

$$g(\gamma) = \alpha, \text{ or equivalently } \gamma = g^{-1}(\alpha), \quad (1)$$

where g^{-1} is the inverse (function) of g.

β is the area bounded by the lines $y=\alpha$, $x=\mu$ and the curve $y==g(x)$. (See Fig. 3).

Hence:

$$\beta = \int_{\gamma}^{\mu} (g(x) - \alpha)dx \tag{2}$$

giving

$$\beta = G(\mu) - G(\gamma) - \alpha(\mu - \gamma) \tag{3}$$

where the function G is the anti-derivative of g.

This equation can be simplified further by defining $H(x) = G(x) - \alpha x$, the anti-derivative of $g(x) - \alpha$. So Eq. 3 becomes

$$H(\mu) = \beta + H\left(g^{-1}(\alpha)\right) \tag{4}$$

Since H has an inverse function H^{-1}, the expected FFD, μ, must satisfy

$$\mu = H^{-1}\left(\beta + H\left(g^{-1}(\alpha)\right)\right) \tag{5}$$

Special cases

Linear temperature rise

Here, $g(x) = mx + c, \gamma = \frac{\alpha - c}{m}, G(x) = \frac{1}{2}mx^2 + cx, H(x) = \frac{1}{2}mx^2 + (c - \alpha)x$, and since the function H is quadratic, its inverse function H^{-1} must involve a square root. So we have

$$\mu = \sqrt{\frac{2\beta}{m}} + \frac{\alpha - c}{m} \tag{6}$$

Equation 6 can be solved using standard regression techniques. If desired, non-negative regression (Lawson and Hanson 1974) can be used to force β to be real. Furthermore Eq. 6 can be readily extended to include geographical (e.g. latitude) effects.

Let $\mathrm{lat_k}$=latitude at site k, $\beta_k = \mathrm{P} + \mathrm{Q}\,\mathrm{lat_k}$ and $\alpha_k = \mathrm{R} + \mathrm{S}\,\mathrm{lat_k}$.

Then by putting $\lambda_k = \mu_k + \mathrm{c_k}/\mathrm{m_k}$ we can use a non-linear least-squares procedure (e.g. nls() in the statistical package R/Splus) to estimate the four new model coefficients of P, Q, R and S.

Sine wave

Here $g(x) = A\sin(x + B) + C = \alpha$, which is monotonic increasing, provided $A - C \le \alpha \le A + C$, in which case we must have $g(\gamma) = A\sin(\gamma + B) + C = \alpha$, giving

$$\gamma = \sin^{-1}\left(\frac{\alpha - C}{A}\right) - B$$

Then

$$H(x) = A\cos(x + B) - (c - A)x$$

The inverse of this function is needed to obtain μ (via Eq. 5). But it is not possible to find a closed form for the inverse of this function, which is equivalent to Kepler's equation (Colwell 1993). In practice we use the R/Splus function uniroot() to determine the limits of integration in Eq. 2, and then the R/Splus function optim() to perform a Nelder-Mead optimisation (Nash 1990; Nelder and Mead 1965) and hence make estimates of α and β. (Similar functions provided in many other packages could be similarly employed.)

Photo-period + GDD

If $\theta < \gamma$ or equivalently $\theta < g^{-1}(\alpha)$, then the situation reduces to that already considered.

Otherwise, β is the area bound by the lines $y=\theta$, $y=\mu$, $x=\alpha$, and the curve $y=g(x)$ (See Fig. 3c).

So Eq. 2 becomes

$$\beta = \int_{\theta}^{\mu} (g(x) - \alpha)dx$$

This is the same form as before. We can cover both cases by defining

$$M(\alpha, \theta) = \max\left(g^{-1}(\alpha), \theta\right).$$

Then we must solve the equation

$$H(\mu) = \beta + H(M(\alpha, \theta))$$

Again we chose to use R/Splus, where the function uniroot() was used to determine the appropriate limits of integration in Eq. 2 (in its modified form given above). Finally the R/Splus function optim() was used to estimate α, β and θ.

More generally, the temperature function $g(x)$ (and all parameters and functions derived from it) varies from year to year. The parameters α, β and θ remain fixed. Given the observed FFDs as estimates of the values of μ from year to year, these unknown parameters can be estimated by the methods described.

References

Abu-Asab MS, Peterson PM, Shetler SG, Orli SS (2001) Earlier plant flowering in spring as a response to global warming in the Washington, DC, area. Biodivers Conserv 10:597–612

Baker CK, Gallagher JN, Monteith JL (1980) Daylength change and leaf appearance in winter wheat. Plant Cell Environ 3:285–287

Bates DM, Chambers JM (1992) Nonlinear models. In Chambers JM, Hastie JM (eds) Statistical models. Wadsworth & Brooks/Cole, Pacific Grove, CA, Chapter 10

Bertero D (2001) Effects of photoperiod, temperature and radiation on the rate of leaf appearance in quinoa (*Chenopodium quinoa* Willd.) under field conditions. Ann Bot-Lund 87:495–502
Cannell MGR, Smith RI (1983) Thermal time, chill days and prediction of budburst in *Picea sitchensis*. J Appl Ecol 20:951–963
Cesaraccio C, Spano D, Snyder RL, Duce P (2004) Chilling and forcing model to predict bud-burst of crop and forest species. Agr Forest Meteorol 126:1–13
Chmielewski FM (1996) The International Phenological Gardens across Europe. Present state and perspectives. Phenol Seasonality Modell 1:19–23
Chuine I, Cour P, Rousseau DD (1998) Fitting models predicting dates of flowering of temperate-zone trees using simulated annealing. Plant Cell Environ 21:455–466
Colwell P (1993) Solving Kepler's equation over three centuries. Willmann-Bell, Richmond, VA
Degrandi-Hoffman G, Thorp R, Loper G, Eisikowitch D (1996) Describing the progression of almond bloom using accumulated heat units. J Appl Ecol 33:812–818
De Melo-Abreu JP, Barranco D, Cordeiro AM, Tous J, Rogado BM, Villalobos FJ (2004) Modelling olive flowering date using chilling for dormancy release and thermal time. Agr Forest Meteorol 125:117–127
Epperson BK (1993) Recent advances in correlation studies of spatial patterns of genetic variation. Evol Biol 27:95–155
Epperson BK, Clegg MT (1986) Spatial autocorrelation analysis of flower color polymorphisms within substructured populations of morning glory (*Ipomoea purpurea*). Am Nat 128:840–858
Escudero A, Iriondo JM, Torres E (2003) Spatial analysis of genetic diversity as a tool for plant conservation. Biol Conserv 113:351–365
Falusi M, Calamassi R (1990) Bud dormancy in beech (*Fagus sylvatica* L.). Effect of chilling and photoperiod on dormancy release of beech seedlings. Tree Physiol 6:429–438
Fitter AH, Fitter RS (2002) Rapid changes in flowering time in British plants. Science 31:1689–1691
Fitter AH, Fitter RSR, Harris ITB, Williamson MH (1995) Relationships between first flowering date and temperature in the flora of a locality in central England. Funct Ecol 9:55–60
Hänninen H (1990) Modeling bud dormancy release in trees from cool and temperate regions. Acta Forestalia Fennica 213:1–47
Heide OM (1993) Daylength and thermal time responses of budburst during dormancy release in some northern deciduous trees. Physiol Plantarum 88:531–540
Heywood JS (1991) Spatial analysis of genetic variation in plant populations. Annu Rev Ecol Syst 22:335–355
Hodgson AS (1978) Rapeseed adaptation in northern New South Wales. I. Phenological responses to vernalisation, temperature and photoperiod by annual and biennial cultivars of *Brassica campestris* L. *Brassica napus* L. and wheat cv. Timgalen. Aust J Plant Physiol 29:693–710
IPCC (Intergovernmental Panel on Climate Change) (2001) Climate change 2001: the scientific basis. Cambridge University Press, Cambridge
Landsberg JJ (1974) Apple fruit bud development and growth; analysis and an empirical model. Ann Bot-Lund 38:1013–1023
Lauscher AUF, Printz H (1955) Die Phänologie Norwegens. Teil I. Allgemeine Übersicht. Skrifter, Det Norske Videnskaps-Akademi i Oslo. I. Mat-Naturv Klasse 1955 1:1–99
Lawson CL, Hanson RJ (1974) Solving least squares problems. Prentice-Hall, Englewood Cliffs, NJ
Menzel A, Fabian P (1999) Growing season extended in Europe. Nature 397:659
Minin AA (2000) Phenology of Russian plain: data and generalisations (in Russian). ABF, Moscow
Mitchell TD, Carter TR, Jones PD, Hulme M, New M (2004) A comprehensive set of high-resolution grids of monthly climate for Europe and the globe: the observed record (1901–2000) and 16 scenarios (2001–2100). Tyndall Centre Working Paper 55. Tyndall Centre, Norwich, UK
Murray MB, Cannell MGR, Smith RI (1989) Date of budburst of fifteen tree species in Britain following climatic warming. J Applied Ecol 26:693–700
Myers LF, Christian KR, Kirehner RJ (1982) Flowering responses of 48 lines of oilseed rapes (*Brassica* spp.) to vernalisation and daylength. Aust J Agr Res 33:927–936
Nash JC (1990) Compact numerical methods for computers. Linear algebra and function minimisation. Adam Hilger, Bristol
Nelder JA, Mead R (1965) A simplex algorithm for function minimization. Comput J 7:308–313
Reaumur RAF de (1735) Observations du thermometre, faites a Paris pendant l'annee, compares avec celles qui ont ete faites sous la ligne, a l'lsle de France, a Alger et en quelques-unes de nos isles de I' Amerique. Mem Acad des Sci, Paris 545
Salisbury FB (1963) The flowering process. Macmillan, New York
Slafer GA, Rawson HM (1994) Sensitivity of wheat phasic development to major environmental factors: a re-examination of some assumptions made by physiologists and modelers. Aust J Plant Physiol 21:393–426
Slafer GA, Rawson HM (1995) Deveolpment in wheat as affected by timing and length of exposure to long photoperiod. J Exp Bot 46:1877–1886
Sparks TH, Jeffree EP, Jeffree CE (2000) An examination of the relationship between flowering times and temperature at the national scale using long-term phenological records from the UK. Int J Biometeorol 44:82–87
Theurillat JP, Guisan A (2001) Potential impact of climate change on vegetation in the European Alps: a review. Climatic Change 50:77–109
Thomson AJ, Moncrieff SM (1981) Prediction of budburst in Douglas-fir by degree-day accumulation. Can J For Res 12:448–452
Trudgill DL, Honek A, Li D, Van Straalen NM (2005) Thermal time-concepts and utility. Ann Appl Biol 146:1–14
Welling A, Rinne P, Vihera-Aarnio A, Kontunen-Soppela S, Heino P, Palva ET (2004) Photoperiod and temperature differentially regulate the expression of two dehydrin genes during overwintering of birch (*Betula pubescens* Ehrh.). J Exp Bot 55:507–516